Radial Microbrain (Micrencephaly) Is Caused by a Recurrent Variant in the RTTN Gene

Clarisse Gins, Fabien Guimiot, Séverine Drunat, Clemence Prévost, Jonathan Rosenblatt, Yline Capri, Pascaline Letard, Suonavy Khung-Savatovsky, Mohamed Amine Mahi Henni, Siham Chafai Elalaoui, et al.

RESEARCH ARTICLE OPEN ACCESS

Radial Microbrain (Micrencephaly) Is Caused by a Recurrent Variant in the *RTTN* Gene

Clarisse Gins,[1] Fabien Guimiot,[2,3] Séverine Drunat,[2,4] Clemence Prévost,[2] Jonathan Rosenblatt,[5] Yline Capri,[6] Pascaline Letard,[3] Suonavy Khung-Savatovsky,[3] Mohamed Amine Mahi Henni,[7] Siham Chafai Elalaoui,[8] Marianne Alison,[2,9] Sophie Guilmin Crepon,[10] Pierre Gressens,[2] Alain Verloes,[2,6] Renata Basto,[11] Vincent El Ghouzzi,[2] and Sandrine Passemard[1,2]

Correspondence
Dr. Passemard
sandrine.passemard@aphp.fr

Neurol Genet 2025;11:e200221. doi:10.1212/NXG.0000000000200221

Abstract

Background and Objectives

Genetic primary microcephaly (PM) is a defect in early brain development leading to congenital microcephaly, mostly recessively inherited, and mild-to-moderate intellectual disability. PM has been largely elucidated, thanks to exome and genome sequencing. However, radial microbrain, the most severe form of genetic PM or micrencephaly described in the 1980s, which leads to early lethality or very severe intellectual handicap, remains without a molecular diagnosis. We sought to identify the cause of radial microbrain by analyzing the genotype of children/adults and fetuses with an extremely small brain.

Methods

We searched for individuals with the smallest head circumference among patients with a confirmed diagnosis of PM included in 2 French and European observational studies coordinated at the Robert Debré Children's Hospital in Paris. Their neurodevelopment and brain imaging were analyzed, as well as next-generation sequencing for a panel of microcephaly genes or exome sequencing. Neuropathologic and immunohistologic analyses of extremely severe microcephalic fetal brains and stage-matched controls were performed. A nonparametric test and Mann-Whitney post-test were used to compare the cortical thickness between groups.

Results

We identified 5 individuals (4 female patients, 7 years 10 months–19 years) with a particularly small brain among a series of 50, all suffering from a severe neurodevelopmental disorder with no ability to communicate verbally and, in 3 of them, no ability to walk. Genetic analysis revealed in all individuals the presence of the same homozygous variant c.2953A>G (p.R985G) in the *RTTN* gene (ROTATIN). The same variant was found in 2 fetuses whose neuropathologic evaluation showed a major reduction in the thickness of the ventricular zone and neuronal heterotopias. The cortical plate was reduced by 70% compared with controls, irrespective of the region considered. Immunostaining with vimentin showed a 50% loss of radial glial columns, characteristic of radial microbrain.

Discussion

Our data show that the homozygous c.2953A>G substitution in *RTTN* is a recurrent variant responsible for radial microbrain, the most severe form of primary microcephaly. Our combined neurologic, imaging, and histopathologic approaches provide a better understanding of the severity of this condition and its prognosis.

[1]Service de Neurologie Pédiatrique, DMU INOV-RDB, APHP, Hôpital Robert Debré, Paris, France; [2]Université Paris Cité, Inserm UMR 1141, NeuroDiderot, Paris, France; [3]Département de Génétique, UF de fœtopathologie, DMU BIOGE'M, APHP, Hôpital Robert Debré, Paris, France; [4]Département de Génétique, UF de Génétique Moléculaire, DMU BIOGE'M, APHP, Hôpital Robert Debré, Paris, France; [5]Unité de Médecine Foetale, DMU Gynécologie Périnatalité, APHP, Hôpital Robert Debré, Paris, France; [6]Département de Génétique, UF de Génétique Clinique, DMU BIOGE'M, APHP, Hôpital Robert Debré, Paris, France; [7]Service de Pédiatrie, Hôpital de Castanel, Oran, Algérie; [8]Département de Génétique Médicale, Institut National d'Hygiène, Rabat, Maroc; [9]Service de Radiologie pédiatrique, APHP, Hôpital Robert Debré, Paris, France; [10]Unité de Recherche Clinique, APHP, Hôpital Robert Debré, Paris, France; and [11]Biology of Centrosomes and Genetic instability, Institut Curie, PSL Research University, CNRS UMR 144, Paris, France.

The Article Processing Charge was funded by Hopital Robert Debré, APHP, Université Paris Cité or INSERM.

Glossary

Array-CGH = array comparative genomic hybridization; **aRGC** = apical radial glial cell; **bRGC** = basal radial glial cell; **CP** = cortical plate; **ES** = exome sequencing; **HC** = head circumference; **IP** = intermediate progenitor; **iSVZ** = inner subventricular zone; **MCPH** = microcephaly primary hereditary; **NGS** = next-generation sequencing; **oSVZ** = outer subventricular zone; **PM** = primary microcephaly; **VZ** = ventricular zone; **WG** = week of gestation.

Trial Registration Information

ClinicalTrials.gov number: NCT01565005.

Introduction

Radial microbrain or micrencephaly is the most severe form of primary microcephaly (PM), a rare condition mostly recessively inherited. Described in 1989 by Philippe Evrard, this extremely small brain, whose weight may not reach 100 g at term rather the expected 500 ± 100 g,[1] owes its name to its impressive neuropathologic characteristics.[2-6,e1,e2]

The marked reduction in the number of radial columns in the fetal telencephalon suggests a drastic reduction in the number of proliferative units, at the very beginning of neurogenesis, during the second month of pregnancy in humans.[7] At this stage, apical radial glial cells (aRGCs), the founder neural progenitors, undergo symmetric proliferative divisions to increase the pool of progenitors in the ventricular zone (VZ).[7-13,e3,e4,e5] Each aRGC forms a radial column or proliferative unit from which will be generated through asymmetric neurogenic divisions, intermediate progenitors (IPs), basal radial glial cells (bRGCs) that will populate the inner subventricular zone (iSVZ) then the outer subventricular zone (oSVZ), and/or neurons, thereby increasing cortical thickness and surface area. Neurons will migrate along parental radial fibers to their final destination in the cortical plate (CP).[14-16] This vertical columnar organization serves as the proliferative unit driving the production of clonally related neurons that will populate the CP before the well-ordered horizontal six-layered cortex appears.[14,15,17]

Radial microbrain often leads to early lethality, due to medically intractable epileptic seizures. Surviving patients show severe intellectual disability without verbal communication.[18] No genetic cause has been yet identified for radial microbrain, unlike less severe but more common PMs. Most PMs (microcephaly primary hereditary, MCPH) are associated with variants affecting proteins (1) of the mitotic spindle apparatus (centrosomal or spindle pole proteins; astral, spindle, or kinetochore microtubules; motor proteins),[19-25,e7-e10] (2) regulating the cell cycle,[26,27] or (3) involved in DNA damage response.[28,29,e11] The most common MCPH disorders are caused by variants in *ASPM*[30,e12] and *WDR62*,[31,e13,e14] 2 genes encoding minus-end microtubule proteins, and in *CDK5RAP2*,[32] a gene encoding a centrosomal protein. MCPH phenotype corresponds to that of the "microcephalia vera" (MV) described in the historical literature, with a less severe clinical and neuropathologic phenotype. *ASPM*-related MCPH is the paradigm of MV, with a borderline IQ, mild-to-moderate intellectual disability, and spared long-term memory compatible with a certain autonomy in daily life.[33] Despite recent progress in identifying genes responsible for MCPH/PM,[20] no variants of these or the many other MCPH/PM-related genes have ever been associated with the radial microbrain.

In this study, we identified a single-nucleotide substitution (c.2953A>G) in *RTTN*, a gene encoding a centrosomal protein involved in centriole duplication and cilia biogenesis,[34] in 5 patients and 2 fetuses and provided the first histopathologic evidence that this recurrent variant previously reported in 4 patients[35-37] is associated with a radial microbrain phenotype. RTTN-related phenotypes were previously known mainly for their association with polymicrogyria and seizures without microcephaly, or microcephaly, short stature and polymicrogyria with or without seizures.[37-42,e15-e19]

Methods

Patient Recruitment

Individuals were part of a French series of 50 microcephalic patients, including 23 previously reported patients, from a single-center prospective, observational, natural history study, conducted between 2014 and 2019 at Robert Debré Hospital, Paris (PHRC, AOM 10147). Parents provided informed consent for their child's participation in the protocol approved by the Paris Research Ethics Committee (P100128) and registered on ClinicalTrials.gov (NCT01565005, MICROFANC, PI: Prof. Sandrine Passemard).

The parents authorized their children to participate in (1) the imaging and clinical examination dedicated to microcephaly and (2) genetic testing. Retrospective clinical data (anthropometric measurements, psychomotor development, brain imaging, and neuropathologic examination) of individuals were collected as part of clinical follow-up.

The 50 patients included in this study between 2014 and 2019 met the clinical inclusion criteria for PM diagnosis.

Figure 1 Clinical and Imaging Data From Patients Carrying the c.2953A>G Variant in the *RTTN* Gene Showing the Severity of Their Phenotype Compared With the Reported Patients

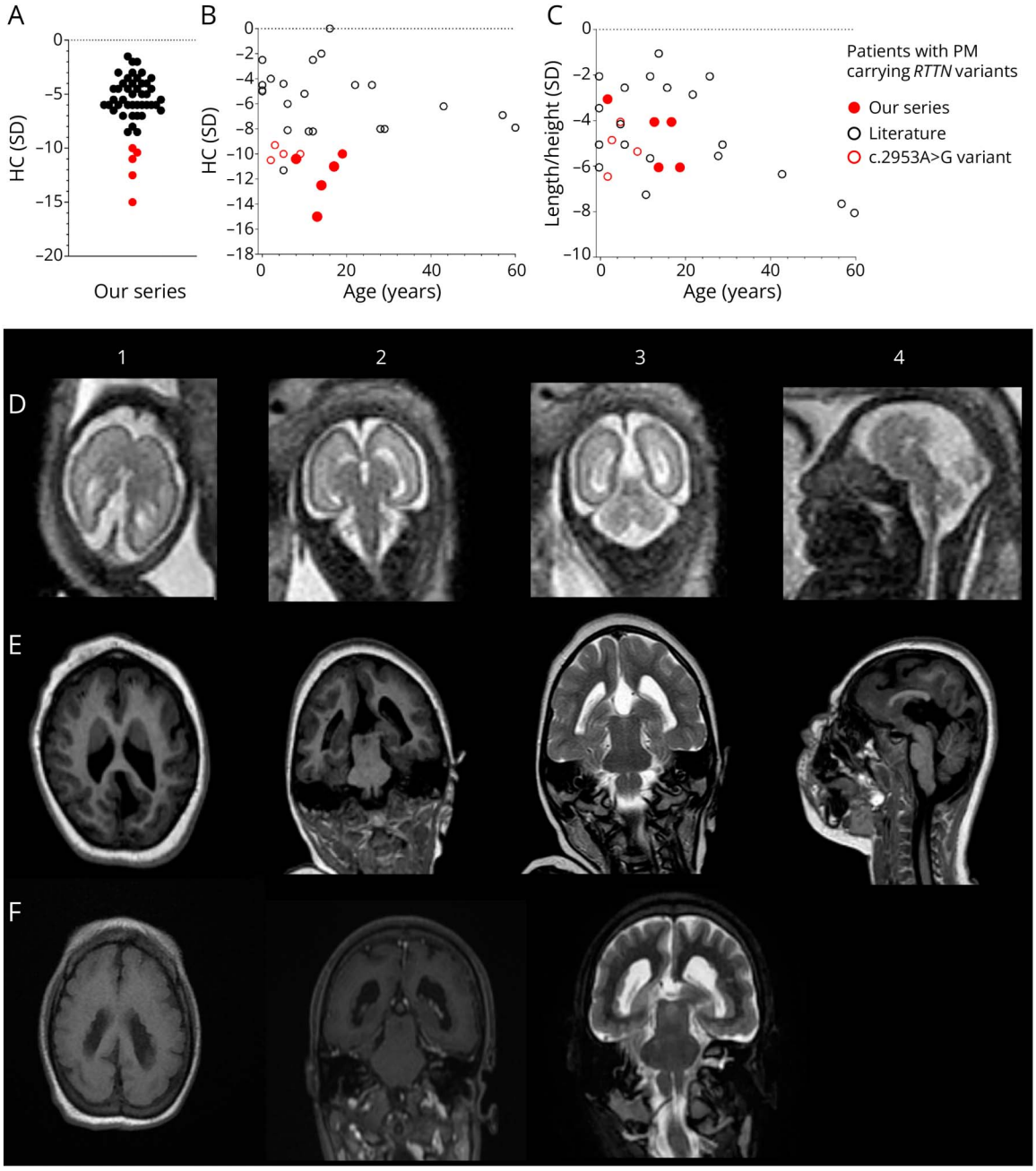

(A) Head circumference at follow-up of the 50 patients with primary microcephaly enrolled in the Microfanc and Euromicro research projects. Red dots indicate head circumference <−10 SD in the 5 patients included in this study. (B and C) HC (B) and height (C) of reported patients with RTTN-related phenotypes. The empty round symbol represents individuals carrying the c.2953A>G variant in the *RTTN* gene: previously reported patients in black and those in our series in red. (D) Brain MRI with axial, coronal, and sagittal T2-weighted images performed in the third trimester of pregnancy showing the lissencephalic appearance of the cortex at WG 32 (D1-3), the hypoplasia of the corpus callosum, and the interhemispheric cyst (D4). (E) Brain MRI with axial and coronal T1-weighted (E1-2) and coronal and sagittal T2-weighted images (E3-4) performed at the age of 6 showing a simplified gyral pattern of the cortex (E1-3), periventricular neuronal heterotopia, hypoplasia of the corpus callosum, and an interhemispheric cyst (E4). (F) Brain MRI (F) with axial and coronal FLAIR (F1-2) and coronal and sagittal T2-weighted images (F3-4) performed at the age of 14 showing a simplified gyral pattern of the cortex and periventricular neuronal heterotopia (F1-3).

Inclusion criteria were (1) age older than 3 years, (2) access to French social security, (3) no contraindication for MRI, (4) head circumference less than or equal to −2 SD at birth and −3 SD after 6 months of age according to the WHO growth charts[43], and (5) PM without gross malformation inside or outside the CNS.

The medical history of the pregnancy and growth parameters at birth and at follow-up, including weight, height, and head circumference, were recorded. Patients underwent brain imaging and neuropsychological assessment. All patients underwent a similar clinical evaluation and brain imaging.

Table 1 Clinical, Neurologic, Behavioral, and Imaging Findings of Patients From Our Series and Previous Reports Carrying the c.2953A>G Variant in *RTTN* Gene

	Our series	Previous reports[35-37]
No. of patients	5	4
Sex	4 female, 1 male	2 female, 2 male
Pregnancy		
Prenatal detection of microcephaly (trimester of pregnancy)	N = 3 (second T: n = 1, third T: n = 2)	N = 1 (second T: n = 1, data NA for 3)
Birth		
Gestational age, mean (range), weeks	40.5 (39.9 to 41)	39.9 (38.9 to 41)
Birth weight, mean (range), kg	2.27 (1.85 to 2.6)	2.54 (2.27 to 3)
Birth length, mean (range), cm	41.5 (42 to 43)	44.66 (43 to 47)
Birth HC, mean (range), cm	30.3 (27 to 32)	27.12 (26.5 to 28)
At inclusion/last examination		
Mean age (range), y	14.2 (7.9 to 19)	4 (1.8 to 9.5)
Weight, mean (range), SD	−4.05 (−4 to −2.7)	−3.6 (−5.3 to 0)
Height, mean (range), SD	−4.92 (−6 to −4)	−5.3 (−6.4 to −4)
HC, mean (range), SD	−11.68 (−15 to −10)	−8.95 (−10.4 to −6)
Gross motor skills, N, mean age at acquisition (range), y		
Sitting up alone	N = 4, 2.94 (0.83 → 8)	N = 3 (1.8 → ?)
Walking alone	N = 2, 3.33 (1.66 → 5)	N = 1 (1.7)
Fine motor skills		
Grasping objects	N = 5	NA
Thumb-index pinch	N = 1	NA
Language kills		
Babbling	N = 2	NA
Words	N = 0	N = 0
Communication/sociability		
Smiling on response	N = 5	N = 2
Pointing	N = 3	NA
Response to name	N = 0	NA
Autonomy		
Eating alone	N = 0	NA
Getting dressed alone	N = 0	NA
Taking a shower alone	N = 0	NA
Danger awareness	N = 0	NA
Can be left alone at home for 5 min	N = 0	NA
Behavior		
Aggressive behavior	N = 0	N = 1
Self-injury	N = 1	N = 1
Sleep disorders	N = 1	NA

Continued

Table 1 Clinical, Neurologic, Behavioral, and Imaging Findings of Patients From Our Series and Previous Reports Carrying the c.2953A>G Variant in *RTTN* Gene *(continued)*

	Our series	Previous reports[35-37]
Epilepsy	N = 1 (medically refractory epilepsy)	N = 1
Nonepileptic abnormal movements		
Stereotyped movements	N = 5	N = 1
Fascination for his/her hands	N = 5	NA
Brain MRI (4 of 5 individuals)		
Lissencephaly	N = 2	N = 4
Extreme gyral simplification	N = 2	N = 2
Periventricular/laminar neuronal heterotopia	N = 3	N = 1
Interhemispheric cyst	N = 1	N = 1
Corpus callosum agenesis/hypoplasia	N = 3	N = 2
Lobar holoprosencephaly	N = 1	N = 0

Abbreviations: HC = head circumference; N = number of patients with specific features/characteristics among the 5 patients from our series (first column) or 4 patients previously reported (second column); NA = not available.

This research was open to our European collaborators from 2014 to 2018 and funded by ERA-NET grant (ANR-13-RARE-0007-01).

Individuals may participate for a maximum of 2 days over a single period in the year after the signing of the consent form.

The primary outcome measure included comparison of neurologic phenotype and cognitive functioning of patients with PM with different genotypes.

Secondary outcome measures were as follows: (1) establish a clear organizational chart for the diagnosis of PM from the detailed description of the patients' phenotypes and (2) establish epidemiologic data on the molecular causes involved in PM.

Fetal Exploration for Diagnostic and Research Purposes

Parents of fetuses whose pregnancy was terminated for severe microcephaly in the second or third trimester have given their consent for autopsy and neuropathologic and immunohistologic analyses.

Fetuses were selected because of an HC < first percentile based on the French College of Fetal Ultrasound (CFEF, 2006) and were molecularly investigated to bring genetic counseling to families and research (MiCMAC, ANR, 22-CE16-0008).

Molecular Investigations

After ruling out any chromosomal rearrangements by array comparative genomic hybridization (Array-CGH), causal variants were identified by either next-generation sequencing (NGS) on our panel of 200 PM genes or exome sequencing (ES) in the genetic department, at Robert Debré Hospital.

NGS was performed in accordance with the manufacturer's instructions and a protocol developed in-house. This consisted of multiplex PCR enrichment on microfluidic support (Access Array, Fluidigm Corporation) and 2 × 150-bp sequencing with an Illumina MiSeq system. Sequencing reads were mapped in the UCSC Genome Browser (hg19) using MiSeq analysis software, Burrows-Wheeler proofreader, and a genome analysis kit. The exon coverage was 99%. Variants were filtered based on minor allele frequency threshold (<0.005), dbSNP, 1000 Genomes, the NHLBI ESP Exome Variant Server, and an internal data set. Rare variants were annotated for functional characteristics of coding regions using publicly available databases (Polyphen2, SIFT, Variant Tester, and Align GVGD). Variants identified by NGS and segregation among family members were confirmed by Sanger sequencing. Homozygosity mapping was conducted using an SNP array, as shown in the SurePrint G3 Human Genome CGH + SNP Microarray kit (Agilent Technologies).

Brain MRI

Coronal and axial T1-weighted and T2-weighted images were acquired on Sigma, Philips, or GE HealthCare 1.5T scanners for 4 of the 5 patients. In addition, one patient had a T1-weighted 3D sequence with millimeter slices.

Neuropathologic Analysis

Neuropathologic analysis was performed at Robert Debré Hospital. Microcephalic fetal brains and stage-matched normal miscarried fetuses (week of gestation [WG] 16 and WG

21) were fixed in 10% formalin-zinc buffer solution for 1–2 weeks. Macroscopic examination of fetal brains and biometric measurements were compared with the reference atlas according to Fees Higgins Clarke and Larroche.[e20] Fetal brains were paraffin embedded. Hematoxylin-eosin staining was performed on 7-µm paraffin-embedded sections.

Immunohistochemistry

Immunohistochemistry was performed with a Benchmark IHC autostainer (Ventana, Roche) according to the manufacturer's protocols using antibody against vimentin (790-2917, Roche). Sections were counterstained with Mayer's hemalun solution.

Microscopy

Hematoxylin-eosin staining and vimentin immunohistochemistry were analyzed using an Upright Leica DM6B, equipped with an XY motorized stage microscope. Images were acquired through ×2.5, ×10, ×20, or ×40 objectives with a sCMOS camera (Orca Flash 4.0 V2, Hamamatsu, Japan). Acquisitions were performed using Metamorph (MolecularDevices). VZ and CP thickness measurements were obtained using Fiji.[e21]

Statistical Analysis

A nonparametric test followed by the Mann-Whitney post-test was applied to compare the variable "thickness" (cortical or VZ) and number of columns per surface unit, between fetal groups (microcephalic and stage-matched controls). $p < 0.05$ was considered significant.

Data Availability

Data are available on request.

Results

Identification of a Particularly Severe Subgroup of Patients With PM Carrying a Common Variant in the *RTTN* Gene

In our French series of 50 microcephalic patients, the HC of 5 patients very significantly differed from the median at −5.75 SD and mean at −5.83 SD ± 2.66 (CI −5.06/−6.6, Figure 1A) as it exceeded −10 SD after age 6, characteristic of an extreme microcephaly, i.e., micrencephaly (Figure 1, A and B and Table 1). Four of these patients were female. The median age was 14.2 years (range: 7.9–19 years).

These patients had a similar natural history with the following characteristics: (1) early detection of microcephaly, either during the second or third trimester of pregnancy for the 3 youngest patients or at birth for the other 2; (2) intrauterine growth retardation with reduced height, ranging from −3 SD to −6 SD during childhood (Figure 1C and Table 1); (3) extreme gyral simplification on brain MRI, detectable at WG 30 for one (Figure 1, D–F and Table 1), which even resembled microlissencephaly in 2 patients (Figure 1, D–F), associated with neuronal heterotopias, forming laminar nodular or periventricular heterotopia (Table 1 and Figure 1. E and F), and a constant partial agenesis of the corpus callosum; and (4) very severe developmental delay in all patients. In more detail, 3 patients never acquired independent walking and the other 2 patients were able to achieve independent walking (20 months for one and at 5 years for the other). None of the patients were able to communicate verbally. Two patients were able to convey their needs and desires through gestures. One patient exhibited behavioral disorders, with self-harm linked to anxiety and aggressiveness. Stereotyped, nonepileptic movements were reported in all patients, accompanied by a fascination for their hands. One patient was treated for epilepsy. None of the patients were independent in activities such as eating, dressing, and cleaning until late childhood or even adulthood (Table 1).

Unexpectedly, a single variant NM_173630.4 (*RTTN*): c.2953A>G in exon 23 (NP_775901.3:p.R985G) was found in all 5 patients by NGS/ES in the homozygous state. Initially reported by Grandone et al.,[35] this variant (NM_173630.3 (*RTTN*):c.2953A>G located in exon 23) results in the conversion of an arginine into a glycine residue and affects exon 23 splicing, leading to 2 abnormal products: one lacking exon 23 and the other lacking exons 22 and 23 (in Discussion). The variant has been already reported in 4 children and now represents 11 cases so far including those in our series (Tables 1 and 2 and eTable 1), likely creating an ancestral recurrent variant.

The c.2953A>G Variant Results in a Radial Microbrain Phenotype

To understand what early developmental defect might lead to this extreme microcephaly (micrencephaly), we screened our fetal series for variants in *RTTN* and identified 2 fetuses with a severe second trimester microcephaly carrying the same variant.

Neuropathologic analysis of both fetuses revealed a major reduction in brain weight compared with stage-matched controls at WG 16 and WG 21 (71% and 82%, respectively, Table 2) and size at the macroscopic level irrespective of the brain region examined (Figure 2, A–AA). In addition, several brain malformations were observed, including agenesis of the corpus callosum (Figure 2, G–I, Y), fusion (Figure 2, I, V, X) of thalami, and nodular periventricular heterotopia (Figure 2, J–K, Z).

To quantify the reduction in brain size, we measured the thickness of the VZ and CP in different lobes in both fetuses carrying the c.2953A > G *RTTN* variant. The reduction in VZ thickness was evident in all regions at WG 16. A highly significant reduction in VZ was observed in the frontal and parietal lobes, with a reduction of 85% and 86%, respectively, compared with the mean value of the WG 16 matched control (Figure 3, C and D). A similar VZ reduction was observed in the frontal, parietal, and occipital regions (79%, 69%, and 72% reduction, respectively), compared with the mean value of the WG 21 matched control.

Table 2 Clinical, Imaging, and Neuropathologic Findings of Fetuses From Our Series Carrying the c.2953A > G Variant in *RTTN* Gene

Sex	Male	Male
Pregnancy		
Prenatal detection of microcephaly (stage of pregnancy), weeks	15.66	20.33
Pregnancy termination, weeks	16.33	21.33
Fetal examination		
Weight, grams/percentile	150 <<3rd p	385 <<3rd p
Length, cm/percentile	20, 25th p	27, <5th p
HC, cm/percentile	12, <3rd p	15.5, <3rd p
Macroscopic analysis		
Brain weight, grams, percentile	10.1, <<3rd p (50th percentile from a 11.8 WG fetus)	17 (50th percentile from a 14 WG fetus)
Weight of the cerebellum and brainstem, percentile	25th p	NA
Sloping forehead	Yes	Yes
Absence of detectable sylvian fissure or open sylvian fissure	Yes	Yes
Frontal lobe hypoplasia	Yes	Yes
Nondisjunction or remaining fusion of both hemispheres	Yes	Yes
Corpus callosum hypoplasia	Yes	No
Presence of olfactory bulbs	Yes	Yes
Neuropathology		
Microlissencephaly	Yes	Yes
Fusion of thalamic nuclei	Yes	Yes
Periventricular and basal ganglia neuronal heterotopia	Yes	Yes
Septum agenesis	Yes	Yes
Posterior corpus callosum agenesis	No	Yes
Poor density of the VZ	Yes	Yes

Abbreviations: HC = head circumference; NA = not available; VZ = ventricular zone.

Thickness was also reduced significantly and homogeneously across all cortical regions in both fetuses carrying the c.2953A > G *RTTN* variant, with 69%, 72%, and 89% reduction in frontal, frontoparietal, and parietal areas, respectively, at WG 16, compared with mean value of the stage-matched control. Similarly, a reduction of 74%, 80%, and 78% was observed, respectively, in the frontal, parietal, and occipital regions at WG 21, compared with mean value of the stage-matched control (Figure 3, A–B, D–F).

Analysis of hematoxylin-eosin–stained sections of the fetuses carrying the c.2953A>G *RTTN* variant at WG 16 revealed a distinctive pattern in the ventricular, subventricular, and intermediate zones, characterized by a low density of glial columns that appeared too clearly visible and separated from each other, compared with that of the stage-matched control. This radial pattern closely resembles the characteristics of the microbrain described earlier by Evrard et al.[2] (Figure 3D).

To further analyze glial columns, we performed immunochemistry using an antibody against VIMENTIN, which stains radial glial processes of aRGCs and bRGCs. The reduction in the number of radial columns was qualitatively evident (Figure 4, A–C). This specific appearance of spaced columns was identified in both the VZ and SVZ. Higher magnifications showed a significant rarefaction of the number of radial columns in the VZ and SVZ at WG 16. Half of the columns were missing, resulting in a significant expansion of the interstitial spaces between the columns compared with a stage-matched control (p = 0.0159, mean of columns per surface: 32.75 ± 1.7 vs 17.6 ± 5.1 in control vs affected fetus,

Figure 2 Neuropathologic Analysis of Fetuses Carrying the c.2953A>G Variants in the *RTTN* Gene Revealing Micrencephaly

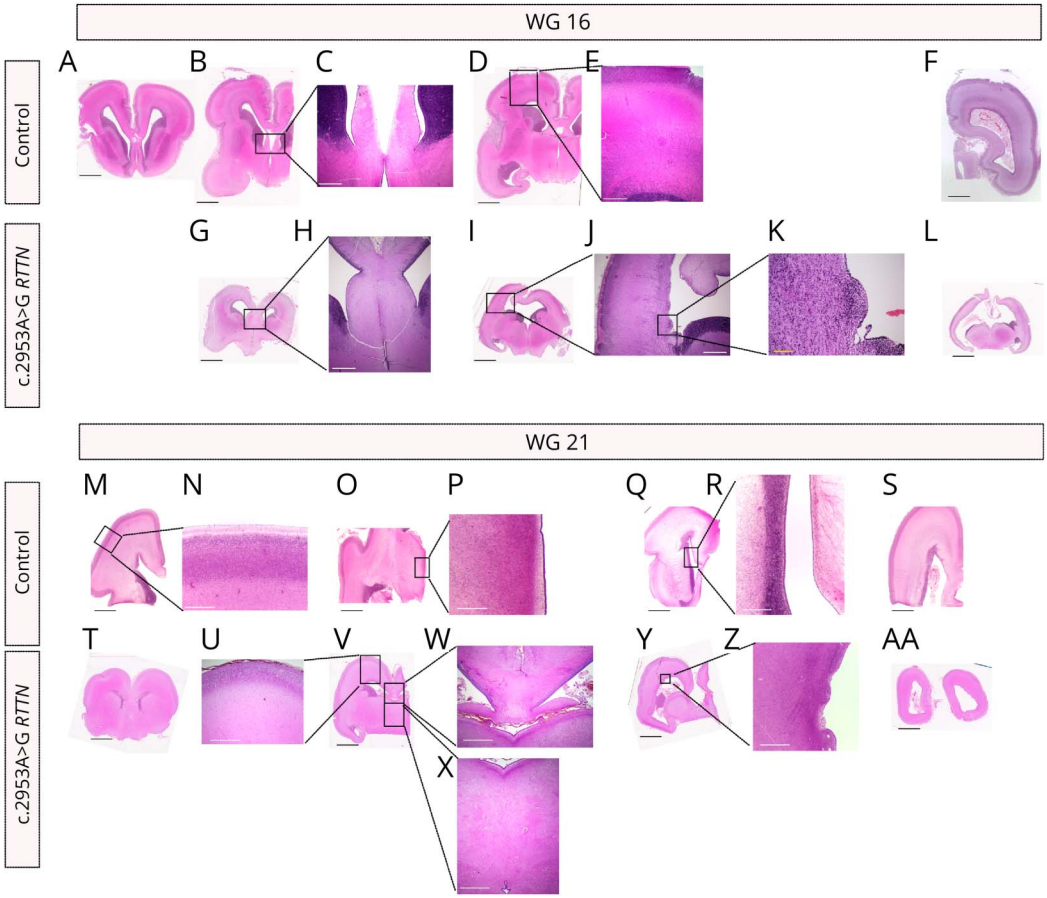

Images of whole-mount histologic preparation (stained with Cresyl violet, imaged using a Leica microscope) of coronal sections. (A–L) Fetus carrying the homozygous c.2953A>G *RTTN* variant (G–L) at WG 16 and stage-matched control (A–F). Control: Staining of a coronal section of both hemispheres in the frontal lobe (A), frontoparietal area (B), parietal lobe (D), and occipital lobe (F). Box area zoom (images 1 and 2) (H&E staining ×40) showing normal separation of both thalami (C) and normal CP (E). RTTN: Staining of a coronal section of both hemispheres in the frontal lobe (G). The intermediate mass between the 2 thalami (H) and in the frontoparietal area (I) can be observed. The posterior corpus callosum hypoplasia responsible for a single posterior ventricle (I) and irregular VZ (J) can be observed. Box area zoom (H&E staining ×40) showing the thalamic fusion on midline with an intermediate mass between the 2 hypoplastic thalamic nuclei (H) and irregular VZ with periventricular heterotopia (J and K). (M–AA) Fetus carrying the homozygous c.2953A>G *RTTN* variant (T–AA) at WG 21 and stage-matched control (M–S). Control: Staining of a coronal section of the left hemisphere in the frontal lobe (M), frontoparietal area (O), parietal lobe (Q), and occipital lobe (S). Box area zoom (H&E staining ×40) showing normal CP (P) and normal VZ (R). RTTN: Staining of a coronal section of both hemispheres in the frontal lobe (T), frontoparietal area (V), parietal lobe (Y), and occipital lobe (AA). Box area zoom (H&E staining ×40) showing a reduction in CP thickness (U), a thalamic fusion on midline with an intermediate mass between the 2 thalami (W and X), and irregular VZ with periventricular heterotopia (Z). Scale bars for A–B, D, F, G, I, L, M, O, Q, S-T, V, Y, AA: 5 mm; for C, E, H, J, N, P, R, U, W, X, Z: 500 µm; and for K: 100 µm.

Figure 4, C and D). Some of these columns were interrupted and did not reach the pia (Figure 4 C).

Discussion

Biallelic *RTTN* variants have been reported in 19 families and 41 individuals, including those in this study. Patients carrying *RTTN* variants exhibit a wide range of phenotypes, from polymicrogyria and seizures without microcephaly, or microcephalic dwarfism, to microcephaly with short stature and brain malformations (polymicrogyria, pachygyria, neuronal heterotopia, pontocerebellar hypoplasia) (eTable 1).

Among these variants, the c.2953A>G (p.R985G) variant affects 25% of cases and has a higher impact on patients' neurodevelopmental abilities. Beyond its molecular effects on mRNA, the consequences of this variant on the dividing cell have not yet been studied, but a close variant (c.2885+8A>G), leading to a truncated protein (p.S963*), has been expressed in RPE1-p53−/− cells.[34] This variant creates a cryptic donor site resulting in retention of 7 base pairs of intron 22 leading to a truncated protein (Ser963*) from exon 22[39] unable to perform its function of promoting procentriole elongation because it fails to convert the primitive procentriole bodies into mature centrioles expressing later-born centriolar proteins such as POC5.[34] The centriole is a cylindrical organelle composed of microtubules and a complex assembly of proteins that contribute to its biogenesis, including its duplication, elongation, and maturation. Two centrioles recruit pericentriolar material and together form the centrosome, the main microtubule-organizing center of mammalian cells,

Figure 3 Histopathologic Analysis Illustrating the Significant Thickness Reduction in the Ventricular Zone and Cortical Plate in the Fetus Carrying the c.2953A>G RTTN Variant

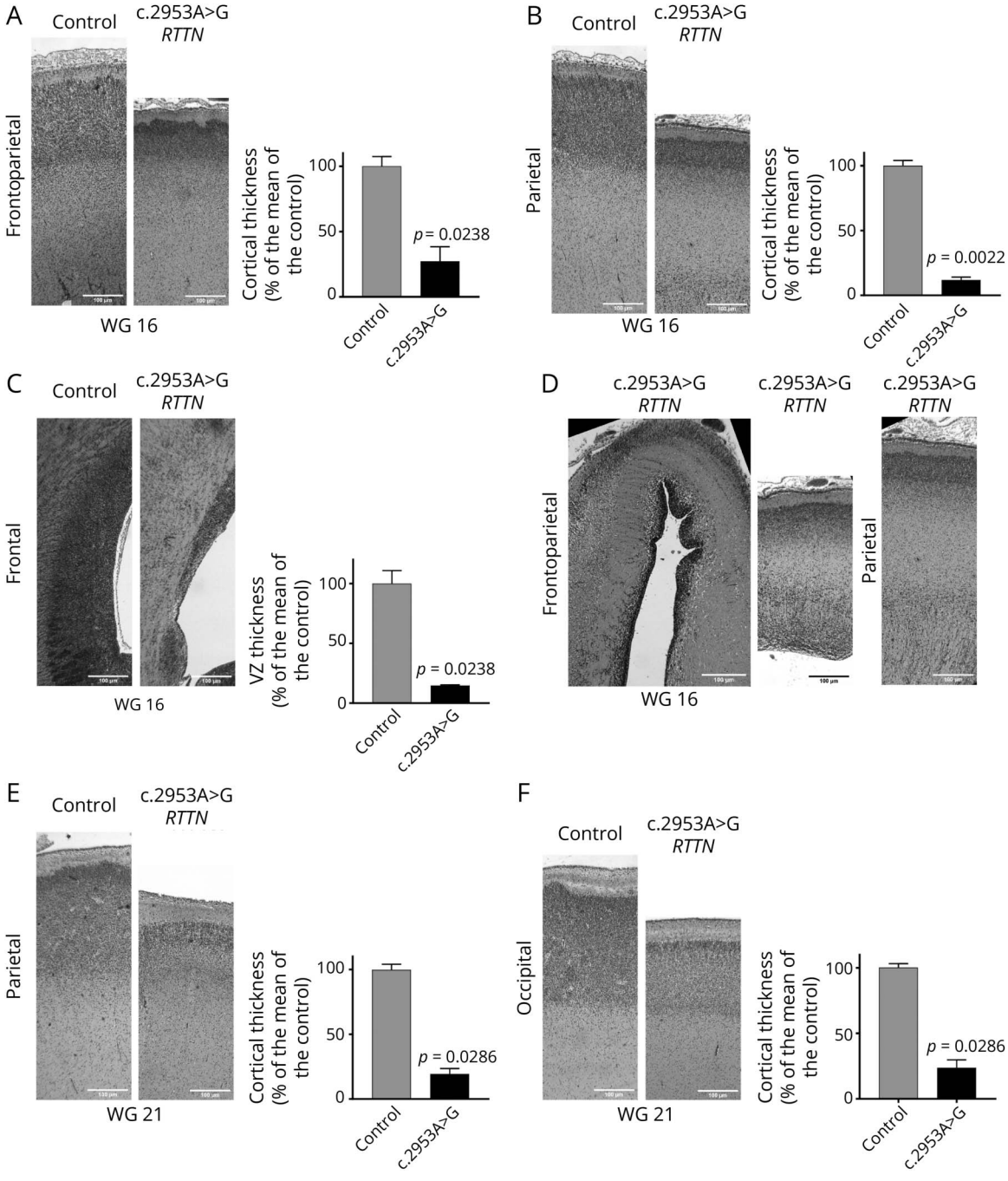

(A–D) Cresyl violet staining of coronal sections of the frontal and parietal cortex of the WG 16 fetus carrying the homozygous c.2953A>G variant in the *RTTN* gene showing the severe reduction of the cortical plate (A–B) and the VZ (C–D) thickness compared with the stage-matched control ($p < 0.05$, nonparametric test, Mann-Whitney post-test). (E–F) Cresyl violet staining of coronal sections of the parietal and occipital cortex of the WG 21 fetus carrying the homozygous c.2953A>G variant in the *RTTN* gene showing the strong reduction of the cortical plate compared with the stage-matched control ($p < 0.0001$, Welch *t* test). Scale bar: 100 µm.

essential for polarity, mobility, and mitotic division (for review, Refs. 44,45,e22). In proliferating cells, the new centriole, also known as procentriole, assembles orthogonally to the proximal part of the 2 existing centrioles. PLK4,[46] SAS6,[47] STIL,[48] and CEP135[49] contribute to the assembly of the procentriole cartwheel, which allow the recruitment of 9 sets of microtubule triplets that elongate to form a more mature centriole. In particular, STIL recruits the CPAP protein necessary for the assembly of the 9 centriolar triplet microtubules[48] from which the centriole can continue to elongate.[50] Once recruited by STIL, RTTN promotes procentriole elongation by recruiting CEP295, which in turn mediates the

Figure 4 The c.2953A>G Variants in the RTTN Gene Cause a Loss of Radial Glial Units Underlying the Radial Microbrain

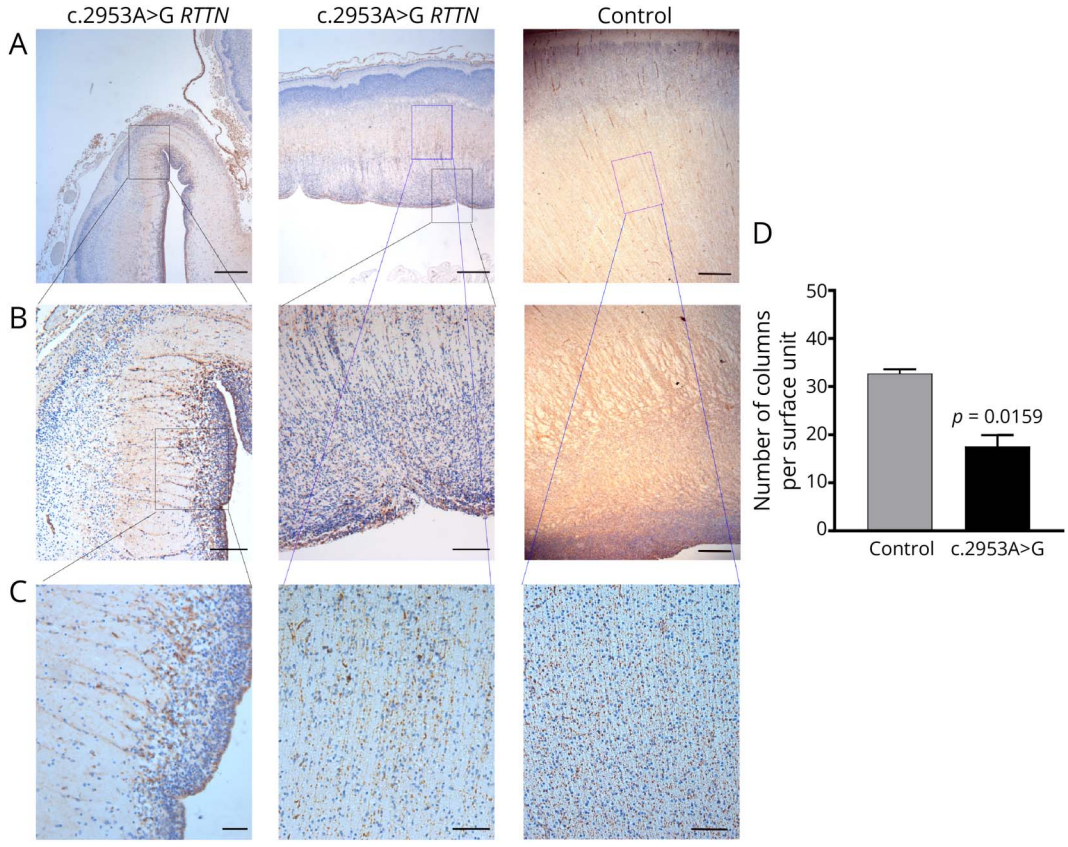

Immunohistochemistry against vimentin of coronal sections of the frontoparietal cortex of the WG 16 fetus carrying the homozygous c.2953A>G variant in the *RTTN* gene (A–C) showing the significant loss of radial glial fibers compared with the stage-matched control ($p = 0.0009$, unpaired *t* test, Figure 3D). Scale bar: 500 µm. Quantification of the number of glial columns per surface unit (66-mm^2 rectangle, 400-µm length).

assembly of the distal half of the centrioles through the loading of POC5 and POC1B.[34]

The c.2953A>G variant is now reported in 6 patients of Moroccan origin (4 previously reported and 2 in our series) and in 5 patients of Algerian origin in our series. Because these countries are very close, this variant is probably an ancestral and recurrent variant. The c.2953A>G variant alters splicing, leading to 2 different transcripts.[35] The first one skips exon 23 but remains in frame and predicts the synthesis of a protein lacking the amino acids encoded by this exon, leading to a truncated protein whose nomenclature would be p.(Ser963_Arg985del). The second loses both exon 22 and exon 23, causing a frameshift and a truncated protein as in the case of the p.S963* protein.[35] Of interest, the c.2885+8A>G variant also skips exon 23 and we can speculate that the truncated protein produced by the loss of exons 22 and 23 loses its ability to promote centriole elongation as well. Comparison of clinical phenotypes indicates that patients with the c.2953A>G variant have a much more severe microcephaly (HC between −9.3 and −10 SD for the 4 patients described previously[35-37] and up to −15 SD for those in this study, mean: −10.97 ± 1.6) than patients with other variants in *RTTN* (HC between 0 and −11.3 SD, mean −5.58 ± 2.6). This highly significant difference in HC between the 2 groups ($p < 0.0001$) allows us to suggest 2 distinct RTTN-related phenotypes: micrencephalies caused by the recurrent c.2953A>G variant, which account for 25% of patients, and other phenotypes including polymicrogyria with normal HC and moderate-to-severe microcephalies caused by variants other than c.2953A>G. Thus, the *RTTN* isoform lacking exon 23 could produce a more stringent effect on neuronal progenitors than the truncated protein from the second transcript of c.2953A>G or c.2885+8A>G variants. The 3 patients carrying the c.2885+8A > G variant had an HC of −8 SD, less reduced than that of patients carrying the 2953A>G (mean: −10.97 ± 1.6), and have so far not been associated with the radial microbrain phenotype in absence of histopathologic analysis. Apart from the 2 fetuses described here, the neuropathologic examination was only performed in 2 other cases but the microbrain phenotype was not reported.[40] More cases and histologic investigation of fetal brains are now required to confirm these hypotheses.

At the cellular level, the radial microbrain likely reflects the extinction of entire columns, which can only be explained by the early death of aRGCs before they generate IPs, bRGCs, and neurons. The mitotic defects observed in RPE1 cells with RTTN variations and P53 loss[51] support this hypothesis. In

these cells, mitotic spindles with abnormal morphology, including multipolar, monopolar, or defective bipolar spindles, are accompanied by excessive aneuploidy and apoptosis.[51] In line with these observations, Pasco Rakic described that in mid-gestation fetal brains (WG 18), up to 30 generations of neurons aligned along a single aRG fiber/process.[e23] The loss of a single radial column can, therefore, have drastic consequences in reducing the capacity of a single aRGC to produce 30 neurons. The loss of half the radial columns would, therefore, compromise the production of half the neurons and consequently 50% of the cortical thickness. The 70% reduction in cortical thickness observed in both fetuses, characterizing the radial microbrain, suggests that additional cellular mechanisms may be involved. Mathematical modeling to identify the number of neurons lost, taking into account the different stages of neurogenesis and in vivo analyses on mutant mice or brain organoids, will help identify the underlying mechanisms involved.

By precisely quantifying the extreme microcephaly (micrencephaly) of 5 patients and studying brain tissues from 2 fetuses, this study provides the first evidence that radial microbrain is caused by a single-nucleotide substitution c.2953A>G variant in the *RTTN* gene responsible for a very severe phenotype in children. Our study shows that clinical and neuropathologic studies remain essential to understand not only the severity of neurodevelopmental disorders but also the mechanisms underlying these phenotypes.

Acknowledgment

The authors acknowledge the patients and their families who have entrusted the care of their children. The authors greatly acknowledge the Cell and Tissue Imaging (PICT-IBiSA), Institut Curie, member of the French National Research Infractucture France-BioImaging (ANR10-INBS-04).

Author Contributions

C. Gins: major role in the acquisition of data. F. Guimiot: major role in the acquisition of data. S. Drunat: major role in the acquisition of data. C. Prévost: major role in the acquisition of data. J. Rosenblatt: major role in the acquisition of data. Y. Capri: major role in the acquisition of data. P. Letard: major role in the acquisition of data. S. Khung-Savatovsky: major role in the acquisition of data. M.A. Mahi Henni: major role in the acquisition of data. S.C. Elalaoui: major role in the acquisition of data. M. Alison: major role in the acquisition of data. S. Guilmin Crepon: major role in the acquisition of data. P. Gressens: drafting/revision of the manuscript for content, including medical writing for content; major role in the acquisition of data. A. Verloes: drafting/revision of the manuscript for content, including medical writing for content; major role in the acquisition of data; study concept or design. R. Basto: drafting/revision of the manuscript for content, including medical writing for content. V. El Ghouzzi: drafting/revision of the manuscript for content, including medical writing for content. S. Passemard: drafting/revision of the manuscript for content, including medical writing for content; study concept or design.

Study Funding

This work was sponsored by the Direction de la Recherche et de l'Innovation, APHP (PHRC - NCT01565005, AOM 10147) and supported by research grants from the French Health Ministry (PHRC National), from the French government managed by the Agence Nationale de la Recherche (EuroMicro, ANR-13-RARE-0007-01; MiCMac, ANR 22-CE16-0008), and as part of the France 2030 program (under the reference ANR-23-IAHU-0010), and from the Université Paris Diderot (DBDD 2014-2018).

Disclosure

The authors report no relevant disclosures. Go to Neurology.org/NG for full disclosures.

Publication History

Received by *Neurology® Genetics* September 20, 2024. Accepted in final form October 22, 2024. Submitted and externally peer reviewed. The handling editor was Stefan M. Pulst, MD, Dr med, FAAN.

References

1. Guihard-Costa A-M, Ménez F, Delezoide A-L. Organ weights in human fetuses after formalin fixation: standards by gestational age and body weight. *Pediatr Dev Pathol*. 2002;5(6):559-578. doi:10.1007/s10024-002-0036-7
2. Evrard P, de Saint Georges P. Pathology of prenatal encephalopathies. In: French JH, Harel S, Casaer P, eds. *Child Neurology and Developmental Disabilities*. Paul H Brookes; 1989.
3. Evrard P. Normal and abnormal development of the brain. In: Rapin I, Segalowitz S, eds. *Handbook of Neuropsychology*. Elsevier; 1992:11-44.
4. Annapurna P, Volpe JJ. Chapter 5 - neuronal proliferation. In: Volpe JJ, Inder TE, Perlman JM, eds. *Volpe's Neurology of the Newborn (Sixth Edition)*. Elsevier; 2018:100-119.
5. Kuzniecky RI, Barkovich AJ. Malformations of cortical development and epilepsy. *Brain Dev*. 2001;23(1):2-11. doi:10.1016/s0387-7604(00)00195-9
6. Jean A. Malformations of the central nervous system in childhood. *Diseases of the Nervous System in Childhood*. Mac Keith Press; 1998:90-91.
7. Rakic P. Developmental and evolutionary adaptations of cortical radial glia. *Cereb Cortex*. 2003;13(6):541-549. doi:10.1093/cercor/13.6.541
8. Mountcastle VB. The columnar organization of the neocortex. *Brain*. 1997;120(Pt 4):701-722. doi:10.1093/brain/120.4.701
9. Mountcastle VB. Introduction. Computation in cortical columns. *Cereb Cortex*. 2003;13(1):2-4. doi:10.1093/cercor/13.1.2
10. Gotz M, Huttner WB. The cell biology of neurogenesis. *Nat Rev Mol Cell Biol*. 2005;6(10):777-788. doi:10.1038/nrm1739
11. Taverna E, Gotz M, Huttner WB. The cell biology of neurogenesis: toward an understanding of the development and evolution of the neocortex. *Annu Rev Cell Dev Biol*. 2014;30:465-502. doi:10.1146/annurev-cellbio-101011-155801
12. Lui JH, Hansen DV, Kriegstein AR. Development and evolution of the human neocortex. *Cell*. 2011;146(1):18-36. doi:10.1016/j.cell.2011.06.030
13. Noctor SC, Martinez-Cerdeno V, Ivic L, Kriegstein AR. Cortical neurons arise in symmetric and asymmetric division zones and migrate through specific phases. *Nat Neurosci*. 2004;7(2):136-144. doi:10.1038/nn1172
14. Torii M, Hashimoto-Torii K, Levitt P, Rakic P. Integration of neuronal clones in the radial cortical columns by EphA and ephrin-A signalling. *Nature*. 2009;461(7263):524-528. doi:10.1038/nature08362
15. Tan SS, Breen S. Radial mosaicism and tangential cell dispersion both contribute to mouse neocortical development. *Nature*. 1993;362(6421):638-640. doi:10.1038/362638a0
16. Rakic P. Specification of cerebral cortical areas. *Science*. 1988;241(4862):170-176. doi:10.1126/science.3291116
17. Buxhoeveden DP, Casanova MF. The minicolumn hypothesis in neuroscience. *Brain*. 2002;125(Pt 5):935-951. doi:10.1093/brain/awf110
18. Ferriero DM, Hemphill JC, Barr R, Evrard P, Gressens P, Barkovich AJ. Severe microcephaly: variant of radial microbrain? *Pediatr Neurol*. 1994;11:127.
19. Marthiens V, Basto R. Centrosomes: the good and the bad for brain development. *Biol Cell*. 2020;112(6):153-172. doi:10.1111/boc.201900090
20. Jayaraman D, Bae B-I, Walsh CA. The genetics of primary microcephaly. *Annu Rev Genomics Hum Genet*. 2018;19:177-200. doi:10.1146/annurev-genom-083117-021441
21. Bettencourt-Dias M, Hildebrandt F, Pellman D, Woods G, Godinho SA. Centrosomes and cilia in human disease. *Trends Genet*. 2011;27(8):307-315. doi:10.1016/j.tig.2011.05.004
22. Nigg EA, Raff JW. Centrioles, centrosomes, and cilia in health and disease. *Cell*. 2009;139(4):663-678. doi:10.1016/j.cell.2009.10.036

23. Marthiens V, Rujano MA, Pennetier C, Tessier S, Paul-Gilloteaux P, Basto R. Centrosome amplification causes microcephaly. *Nat Cell Biol*. 2013;15(7):731-740. doi:10.1038/ncb2746
24. Wimmer R, Baffet AD. The microtubule cytoskeleton of radial glial progenitor cells. *Curr Opin Neurobiol*. 2023;80:102709. doi:10.1016/j.conb.2023.102709
25. Kaindl AM, Passemard S, Kumar P, et al. Many roads lead to primary autosomal recessive microcephaly. *Prog Neurobiol*. 2010;90(3):363-383. doi:10.1016/j.pneurobio.2009.11.002
26. Tingler M, Philipp M, Burkhalter MD. DNA Replication proteins in primary microcephaly syndromes. *Biol Cell*. 2022;114(6):143-159. doi:10.1111/boc.202100061
27. Homem CCF, Repic M, Knoblich JA. Proliferation control in neural stem and progenitor cells. *Nat Rev Neurosci*. 2015;16(11):647-659. doi:10.1038/nrn4021
28. O'Driscoll M. Diseases associated with defective responses to DNA damage. *Cold Spring Harb Perspect Biol*. 2012;4(12):a012773. doi:10.1101/cshperspect.a012773
29. Bianchi FT, Berto GE, Di Cunto F. Impact of DNA repair and stability defects on cortical development. *Cell Mol Life Sci*. 2018;75(21):3963-3976. doi:10.1007/s00018-018-2900-2
30. Bond J, Roberts E, Mochida GH, et al. ASPM is a major determinant of cerebral cortical size. *Nat Genet*. 2002;32(2):316-320. doi:10.1038/ng995
31. Nicholas AK, Khurshid M, Desir J, et al. WDR62 is associated with the spindle pole and is mutated in human microcephaly. *Nat Genet*. 2010;42(11):1010-1014. doi:10.1038/ng.682
32. Bond J, Roberts E, Springell K, et al. A centrosomal mechanism involving CDK5RAP2 and CENPJ controls brain size. *Nat Genet*. 2005;37(4):353-355. doi:10.1038/ng1539
33. Passemard S, Verloes A, Billette de Villemeur T, et al. Abnormal spindle-like microcephaly-associated (ASPM) mutations strongly disrupt neocortical structure but spare the hippocampus and long-term memory. *Cortex*. 2016;74:158-176. doi:10.1016/j.cortex.2015.10.010
34. Chen H-Y, Wu C-T, Tang C-JC, Lin Y-N, Wang W-J, Tang TK. Human microcephaly protein RTTN interacts with STIL and is required to build full-length centrioles. *Nat Commun*. 2017;8(1):247. doi:10.1038/s41467-017-00305-0
35. Grandone A, Torella A, Santoro C, et al. Expanding the phenotype of RTTN variations: a new family with primary microcephaly, severe growth failure, brain malformations and dermatitis. *Clin Genet*. 2016;90(5):445-450. doi:10.1111/cge.12771
36. Cavallin M, Bery A, Maillard C, et al. Recurrent RTTN mutation leading to severe microcephaly, polymicrogyria and growth restriction. *Eur J Med Genet*. 2018;61(12):755-758. doi:10.1016/j.ejmg.2018.08.001
37. Vandervore LV, Schot R, Kasteleijn E, et al. Heterogeneous clinical phenotypes and cerebral malformations reflected by rotatin cellular dynamics. *Brain*. 2019;142(4):867-884. doi:10.1093/brain/awz045
38. Kheradmand Kia S, Verbeek E, Engelen E, et al. RTTN mutations link primary cilia function to organization of the human cerebral cortex. *Am J Hum Genet*. 2012;91(3):533-540. doi:10.1016/j.ajhg.2012.07.008
39. Shamseldin H, Alazami AM, Manning M, et al. RTTN mutations cause primary microcephaly and primordial dwarfism in humans. *Am J Hum Genet*. 2015;97(6):862-868. doi:10.1016/j.ajhg.2015.10.012
40. Chartier S, Alby C, Boutaud L, et al. A neuropathological study of novel RTTN gene mutations causing a familial microcephaly with simplified gyral pattern. *Birth Defects Res*. 2018;110(7):598-602. doi:10.1002/bdr2.1204
41. Stouffs K, Moortgat S, Vanderhasselt T, et al. Biallelic mutations in RTTN are associated with microcephaly, short stature and a wide range of brain malformations. *Eur J Med Genet*. 2018;61(12):733-737. doi:10.1016/j.ejmg.2018.06.001
42. Wambach JA, Wegner DJ, Yang P, et al. Functional characterization of biallelic RTTN variants identified in an infant with microcephaly, simplified gyral pattern, pontocerebellar hypoplasia, and seizures. *Pediatr Res*. 2018;84(3):435-441. doi:10.1038/s41390-018-0083-z
43. World Health Organization. Accessed April 27, 2006. https://www.who.int/tools/child-growth-standards
44. Banterle N, Gönczy P. Centriole biogenesis: from identifying the characters to understanding the plot. *Annu Rev Cell Dev Biol*. 2017;33:23-49. doi:10.1146/annurev-cellbio-100616-060454
45. Gomes Pereira S, Dias Louro MA, Bettencourt-Dias M. Biophysical and quantitative principles of centrosome biogenesis and structure. *Annu Rev Cell Dev Biol*. 2021;37:43-63. doi:10.1146/annurev-cellbio-120219-051400
46. Habedanck R, Stierhof Y-D, Wilkinson CJ, Nigg EA. The Polo kinase Plk4 functions in centriole duplication. *Nat Cell Biol*. 2005;7(11):1140-1146. doi:10.1038/ncb1320
47. Leidel S, Delattre M, Cerutti L, Baumer K, Gönczy P. SAS-6 defines a protein family required for centrosome duplication in C. elegans and in human cells. *Nat Cell Biol*. 2005;7(2):115-125. doi:10.1038/ncb1220
48. Tang C-JC, Lin S-Y, Hsu W-B, et al. The human microcephaly protein STIL interacts with CPAP and is required for procentriole formation. *EMBO J*. 2011;30(23):4790-4804. doi:10.1038/emboj.2011.378
49. Lin Y-C, Chang C-W, Hsu W-B, et al. Human microcephaly protein CEP135 binds to hSAS-6 and CPAP, and is required for centriole assembly. *EMBO J*. 2013;32(8):1141-1154. doi:10.1038/emboj.2013.56
50. Gönczy P. Towards a molecular architecture of centriole assembly. *Nat Rev Mol Cell Biol*. 2012;13(7):425-435. doi:10.1038/nrm3373
51. Chou E-J, Tang TK. Human microcephaly protein RTTN is required for proper mitotic progression and correct spindle position. *Cells*. 2021;10(6):1441. doi:10.3390/cells10061441